

Fragmentation Event Identification Using Back Propagation with Variable Ballistic Coefficient Calculation

Kristen Tetreault¹, Shane D. Ross²

Engineering Mechanics Program, Virginia Tech

Kevin Schroeder³, Jonathan Black⁴

Crofton Dept. of Aerospace and Ocean Engineering, Virginia Tech

ABSTRACT

Sustaining the near Earth environment for future space vehicles and satellites requires an understanding of the past, current, and future space debris population. The leading source of space debris stems from fragmentation, or break-up events. This paper presents a tool with the capability of identifying fragmentation events from two-line element sets pulled from existing space surveillance networks. This fragmentation identification tool determines the objects involved in the fragmentation event using back propagation and particle distribution techniques. Short- and long-term evolution of the fragmentation clouds are studied, as well as the feasibility of determining the location and time of the fragmentation event. A case study on varying the ballistic coefficient is presented to attempt to improve the accuracy of the back propagation and therefore the event identification. A recent February 2018 fragmentation event is analyzed using this technique, with the tool correctly identifying the parent object from the most recent publicly available data.

1. INTRODUCTION

Approximately 13,000 debris pieces larger than 10 cm currently orbit Earth, with scientists estimating that more than 100,000 additional pieces of orbital debris 1-10 cm presently inhabit the near Earth environment [1]. With possibly tens of millions of debris pieces smaller than that, the near Earth environment becomes a dangerously congested place. To sustain this environment for current and future spacecraft, it is critical to increase our knowledge and understanding of the debris population. The leading source of space debris stems from fragmentation, or break-up events. These events are mainly due to either explosions or collisions. Some of these events result in just a few objects that could be short-lived orbiters before re-entering Earth's atmosphere. Others, however, create on-orbit fragments that contribute to the collision risk for satellites and space vehicles operating for a normal lifespan. Continuing to populate the near Earth environment with space debris without understanding the debris population could result in an even more overcrowded space environment encompassing satellite communication problems, navigation problems, and of course, enormous collision risk.

Part of understanding the debris population involves understanding the properties of satellites and their orbital dynamics. Two-line element sets (TLEs) are the most common way of articulating a satellite's orbital properties, and are commonly used for tracking resident space objects. A frequently used term within a TLE is the B^* value. This value is a tuning parameter that influences drag through the ballistic coefficient. Finding an accurate ballistic coefficient from the B^* value can be challenging, as the term can vary widely from one TLE to another for the same satellite. In some cases, the ballistic coefficient will have little to no effect on the satellite's orbit. This occurs when atmospheric drag is not a large concern, as is the case for geosynchronous orbits, or when a satellite has a very small area-to-mass (A/m) ratio. In most other cases, however, finding an accurate ballistic coefficient can greatly increase the accuracy of orbit propagation and determination. Part of this study includes a variation on the calculation method of the ballistic coefficient. Varying the ballistic coefficient, and therefore the A/m ratio, will reveal the intensity of the effect the A/m ratio has on atmospheric drag and solar radiation pressure. This may result in discovering a more

¹ Graduate Student, Engineering Mechanics Program, Virginia Tech, Blacksburg VA 24061

² Professor, Engineering Mechanics Program, Virginia Tech

³ Post-Doctoral Student, Crofton Dept. of Aerospace and Ocean Engineering, Virginia Tech

⁴ Professor, Crofton Dept. of Aerospace and Ocean Engineering, Virginia Tech

efficient and accurate method of calculating the ballistic coefficient for a satellite, which will benefit fragmentation event identification analysis.

This paper presents a tool with the capability of identifying fragmentation events from existing space surveillance networks. Discussion will include a description of the tool, a brief summary of its main functionalities, and an analysis of a recent fragmentation event. The tool calculates the time and location of the event and identifies the true, pre-fragmentation objects involved in the event (commonly referred to as the parent objects). Additionally, variations on the ballistic coefficient calculation are introduced to compare methods in an effort to uncover a more efficient approach to assigning a satellite's ballistic coefficient for orbit propagation.

The tool presented herein is not first of its kind to analyze fragmentation events [2, 3, 4]. However, this tool differs from others in its variation of the ballistic coefficient calculation. This is important in determining the effect the ballistic coefficient has on the A/m ratio, and therefore on the orbital dynamics of the satellite. Determining this effect and its impact on orbital propagation accuracy will help future analyses determine proper accelerations for propagation and consequently, more accurately identified fragmentation events.

2. FRAGMENTATION EVENT

In order to properly test the fragmentation identification tool, a physical fragmentation event was identified for analysis. The 2018 Fregat-SB fragmentation event was chosen as it is the most recent break-up event identified by NASA's Orbital Debris Program Office (ODPO). The ODPO released its quarterly news report in May 2018 describing the details of the Fregat-SB explosion, which occurred 12 February 2018 at approximately 0957GMT \pm 2 minutes [5]. The exploded satellite was a rocket body discarded from the previous launch of a communications satellite. At the time of the explosion, the rocket body was in an orbit of approximately 4070 x 277 km altitude and 50.4 degree inclination [5]. The original rocket body, space surveillance network (SSN) satellite name FREGAT R/B and catalog number 43089, was re-named as a debris piece after the explosion. On 5 March 2018, four additional Fregat-SB debris objects associated with the event were added to the public SSN catalog, pieces 43219-43222. However, the debris associated with SSN number 43221 decayed from orbit less than 10 days after the fragmentation event [5]. Because of this decay, only debris fragments with SSN numbers 43089,43219,43220,43222 were used for propagation and event identification.

3. OVERVIEW OF TOOL

The method used to identify the fragmentation event involves back propagating the debris objects within the fragmentation cloud and computing at each time step the cloud's center of mass (COM), velocity, and the average distance of each fragment to the COM. It is hypothesized that the fragmentation event has occurred when the average distance is at a minimum value. Once the event is identified, the time of the fragment's initial orbit is computed and the COM becomes its location. The parent satellite(s) involved in the event are identified by comparing this computed orbit with a satellite catalog that contains the space population prior to the fragmentation event. For a precise determination of the event, the model uses a special perturbations propagator for the backward propagation. Fig. 1 illustrates the method of the fragmentation event identification tool.

Back propagation techniques have previously provided limited accuracy stemming from errors in the calculation of drag perturbations due to limited knowledge of mass and area [6]. The analysis here introduces variations on the calculation of the ballistic coefficient of each particle in the cloud based on that particle's TLE history stemming directly from the satellite catalog. Three separate calculation methods were analyzed, as well as a scenario in which the ballistic coefficient is not calculated, therefore excluding effects due to drag and solar radiation pressure from the orbital propagator in order to create a control case. Manipulating the ballistic coefficient essentially manipulates the A/m ratio of a satellite, which directly affects atmospheric drag and solar radiation pressure. This direct effect can be seen in Eq. 1 and 2, respectively, which show the calculations for the acceleration due to these effects.

$$a_{drag} = -\frac{1}{2}\rho C_D \left(\frac{A}{m}\right) v_{rel}^2 \frac{\bar{v}_{rel}}{|\bar{v}_{rel}|} \quad (1)$$

$$a_{srp} = -p_{srp} C_R \left(\frac{A}{m}\right) \frac{\bar{r}_{sat}}{|\bar{r}_{sat}|} \quad (2)$$

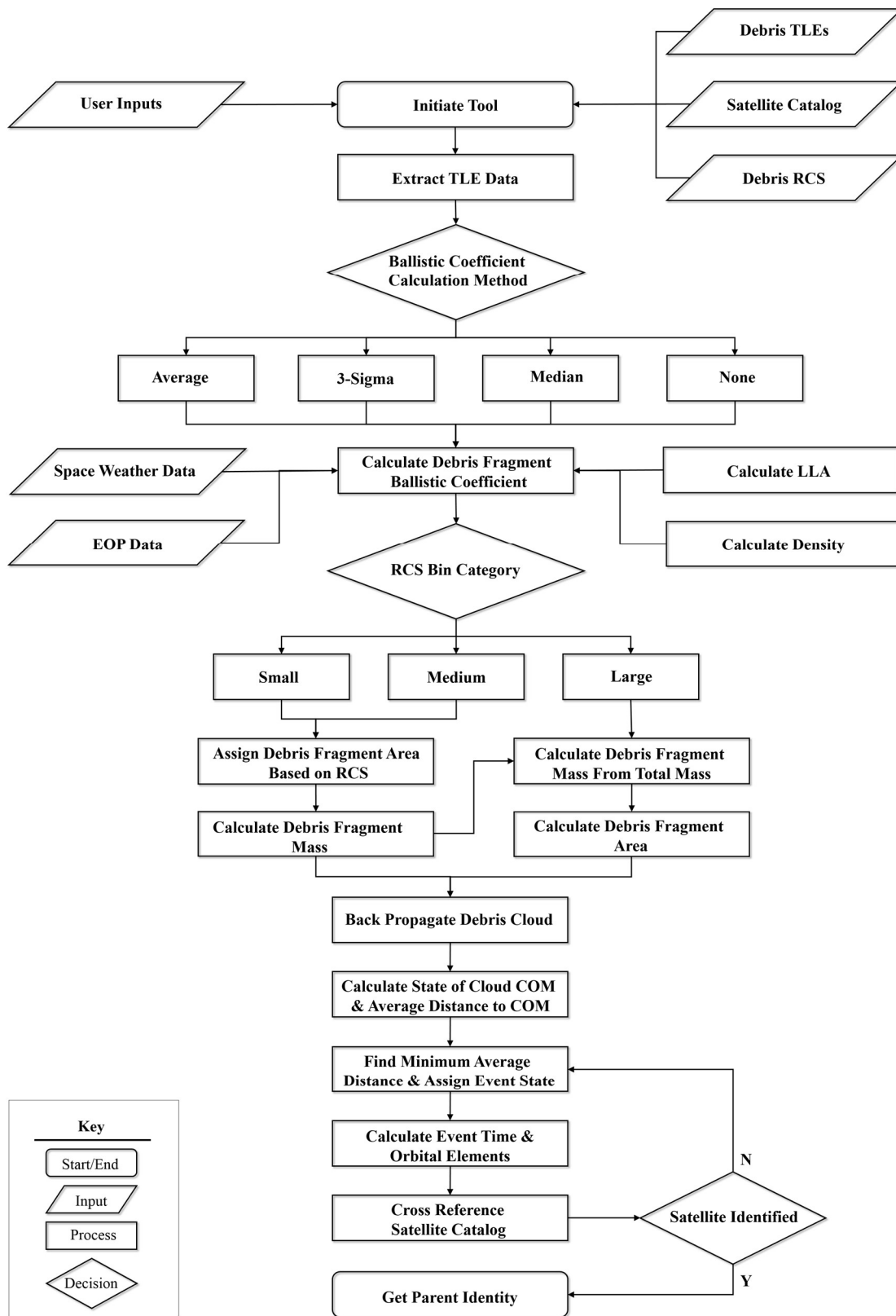


Figure 1: Flow Chart of the fragmentation event identification tool.

For more information on these equations please reference [7]. By manipulating the ballistic coefficient calculation and weighting the particle's area based on the radar cross section (RCS) from the satellite catalog, the accuracy of back propagation can be increased, consequently increasing the accuracy of the fragmentation event identification.

4. DESCRIPTION OF TOOL

The tool initiates by first reading in the debris TLEs, debris RCS, and the satellite catalog directly from the data provided by the Joint Space Operations Center (JSpOC) via space-track.org [8]. The tool also reads in space weather data and earth orientation parameter (EOP) data from information provided by the Center for Space Standards and Innovation via celestrak.com [9]. The debris TLE information is parsed, and one cloud object is created containing the various debris fragments, each with the original assigned TLEs and the extracted information from each TLE. This information is then used to calculate the ballistic coefficient of each debris fragment. Section 5 describes the calculation and variation methodology. Once a value for the ballistic coefficient is established, the area of each debris fragment is approximated based on the RCS of each object using the satellite catalog legend for approximate RCS, shown in Table 1.

Table 1: JSpOC legend for categorizing debris into bins by RCS.

RCS Size Range [m ²]	Bin
RCS < 0.1	Small
0.1 < RCS < 1.0	Medium
1.0 < RCS	Large

Fragments categorized as small and medium are treated differently than fragments categorized as large, as shown in Fig. 1. For fragments categorized as small, the area is taken to be 0.1 m². For medium fragments the area is estimated at 0.45 m². The masses of these fragments are calculated using Eq. 3.

$$m = (BC)C_D A \quad (3)$$

The coefficient of drag, C_D , is assumed to be 2.2, based off a flat plate model [7]. A flat plate is assumed instead of a sphere due to the general nature of fragmentation pieces to more likely be small, flatter objects rather than rounded spheres [10]. Once the masses of small and medium objects are assigned, the mass of fragments categorized as large objects is calculated by totaling the mass from the small and medium fragments and subtracting this from the estimated pre-fragmentation dry mass of the parent object, taken from the ODPO report [11]. If more than one object is categorized as large, the resulting mass is evenly divided between the number of debris fragments. The area for these objects are then backed out by re-working Eq. 3 to calculate area.

Next the debris cloud is propagated backwards in time using Analytical Graphics, Inc. Systems Tool Kit's High-Precision Orbit Propagator (HPOP) [12]. This propagator includes a fourth degree and zeroth order gravitational field (includes J2-J4 perturbations), effects from third-body gravities of the sun and moon, effects due to atmospheric drag, and solar radiation pressure. The effects due to atmospheric drag and solar radiation pressure use the previously calculated mass and area, as well as the assumed coefficient of drag. The effects due to radiation pressure use standard values for the solar radiation pressure coefficient, C_r [13]. This is to allow any effects from ballistic coefficient variation to more easily be identified.

Continuing down the flow chart shown in Fig. 1, the center of mass (COM) of the debris cloud is then calculated at each time step of the propagation. Additionally, each debris fragment's distance to the COM is calculated, and an average of these distances are taken, giving an average debris distance from COM for each time step. It is estimated that the event has occurred once the average distance to the COM is at a minimum. The velocity of the COM is also calculated at each time step.

The tool takes the twenty smallest average distances to the COM and creates an event object guess for each. The position and velocity of the COM at this minimum distance become the estimated position and velocity of the event, and the time step of the guess becomes the event time. From this information, the tool assigns the event Julian date, and then calculates the inclination and semi-major axis of the cloud at the event time. The period is then calculated from the semi-major axis. These orbital elements are chosen as the JSpOC satellite catalog identifies resident space objects by period and inclination.

Once the event time and orbital elements are calculated, the tool cross references the satellite catalog by both inclination and period with a tolerance of ± 0.005 degrees and ± 6 minutes, respectively. Satellites that appear in both searches are then identified as possible parent objects for the fragmentation event. If there are no satellites that appear in both searches, the tool moves onto the next smallest average distance and cross-references again until a parent object is identified.

5. BALLISTIC COEFFICIENT CALCULATION

As previously stated, finding an accurate ballistic coefficient from the B^* value can be challenging, as the term can vary widely from one TLE to another for the same satellite. Fig. 2 depicts the B^* values of all the TLEs for each debris fragment.

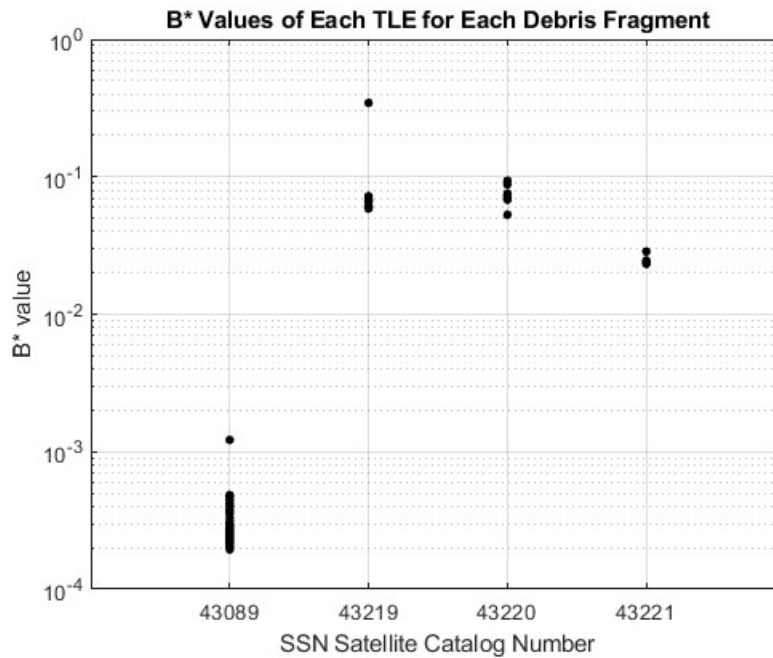


Figure 2: The B^* values taken directly from the TLEs for each debris fragment.

The B^* values for each debris fragment are sometimes clumped together, as in the case of fragment SSN number 43221. However, the other debris fragments are much more spread out. This reiterates the fact that the B^* value is a tuning parameter, and makes finding an efficient method to calculate an accurate ballistic coefficient essential to orbit propagation. This process aims to do just that. After the TLE data for all debris fragments has been extracted, a ballistic coefficient is calculated for each particle within the cloud, as shown in Fig. 1 in the ballistic coefficient decision-making process. First the latitude, longitude, and altitude (LLA) of the fragment is calculated at each TLE epoch. Then the density, ρ , at that LLA is calculated using the nrlmsis00 model [14]. From there, a ballistic coefficient for that TLE is calculated using Eq. 4.

$$BC = \frac{R_{\oplus} \rho}{2B^*} \quad (4)$$

Here, R_{\oplus} is the radius of the Earth. To get a single ballistic coefficient value for each fragment, all the individual ballistic coefficient values from the TLEs for that fragment are used in one of four cases:

- 1) Average - the individual values are averaged
- 2) 3-Sigma - the individual values within 3 standard deviations (3-sigma) of the distribution are averaged
- 3) Median - the median of the individual values is calculated
- 4) None - no ballistic coefficient is calculated and drag is not included in the orbit propagation

Part of this study looks at the difference between these cases and their effects on orbit propagation.

6. FRAGMENTATION ANALYSIS

The fragmentation event identification tool was tested by analyzing the February 2018 explosion of the Fregat-SB satellite. Four total debris pieces were analyzed; debris SSN numbers 43089, 43219, 43220, and 43222. The tool used all available TLEs for each fragment to calculate a ballistic coefficient, and the first available TLE after 23 February 2018 00:00:00.000 for back propagation. The debris fragments 43219-43222 do not include TLEs prior to this date, while the debris fragment 43089 does. For continuity TLEs for back propagation were required to have epochs past this date, while taking the first TLE within this requirement increased the accuracy of the back propagation by decreasing the amount of time required to back propagate. The specific TLE Epochs for each debris fragment can be seen in Appendix A. All debris fragments were back propagated to 01 Jan 2018 00:00:00.000, giving a valuable period of data to parse for a fragmentation event. The total mass of the parent object was assumed to be 340 kg, taken from the ODPO report, and the propagation time step was set to 60 seconds [7].

7. PARENT SATELLITE IDENTIFICATION

The fragmentation event identification tool was able to properly identify the correct parent satellite of the Fregat-SB explosion, SSN number 43089 FREGAT R/B, for two cases of ballistic coefficient calculation, the Average and 3-Sigma cases. In the other two cases, the Median and None case, the tool misidentified the parent object as SSN number 41114 FREGAT DEB, a piece of debris associated with a different Fregat explosion. Table 2 shows the inclination and period of the parent satellite calculated for each case, as well as the actual parent satellite inclination and period taken directly from the satellite catalog.

Table 2: Summary of findings from the tool's analysis of the Fregat-SB fragmentation event to determine a parent satellite. All ballistic coefficient cases are compared against data taken from the JSpOC satellite catalog.

Ballistic Coefficient Case	Guess	Inclination [deg]	Period [min]	Accurately Identified
Average	9	50.4208	124.6235	Y
3-Sigma	9	50.4208	124.6235	Y
Median	19	50.3407	122.9568	N
None	5	50.3405	123.4848	N
Actual	n/a	50.42	130.5	n/a

The calculated inclinations for the Average and 3-Sigma cases were within the ± 0.005 degree tolerance with an error less than 0.005% for both cases. The calculated period of these cases neared the top of the ± 6 minute tolerance, but still stayed within 1% of the actual period. Since both elements were within the tolerance of the actual satellite, the correct parent object was identified.

The inclinations for the Median and None ballistic coefficient cases were only out of the tolerance by about 0.075 degrees, but when considering inclination, this is a large amount. The periods of these cases were much closer to being included in the tolerance, being out by less than two minutes. Though aided by the differences in both orbital elements, the relatively large inclination difference was a greater obstacle to overcome and kept the tool from identifying the correct parent object.

It is important to note that none of the ballistic coefficient cases were able to identify a parent object on their first guess. Recall, each guess corresponds to a minimum average distance to the COM of the cloud. The first guess to identify a parent object becomes the guess associated for that ballistic coefficient case. Looking at the Average case, the 9th smallest average distance to the COM was the first guess to identify a parent object, which was the correct parent satellite. For the Median case, the 19th smallest average distance to the COM was the first guess to identify a parent object, which was an incorrect parent satellite.

8. EVENT TIME IDENTIFICATION

The fragmentation event identification tool was unable to properly identify the correct event time of the Fregat-SB explosion for all four cases of ballistic coefficient calculation. Table 3 shows the event time of the explosion calculated for each case, as well as the actual event time as reported by the ODPO.

Table 3: Summary of findings from the tool's analysis of the Fregat-SB fragmentation event to determine a parent satellite. All ballistic coefficient cases are compared against data reported by the ODPO.

Ballistic Coefficient Case	Event Time
Average	15 January 2018 16:06
3-Sigma	15 January 2018 16:06
Median	22 February 2018 09:10
None	22 February 2018 09:10
Actual	12 February 2018 09:57

The calculated event times are well off the mark of the actual event time. This large error most likely stems from either the atmospheric drag effects on the debris fragments, the method of using the COM to identify the fragmentation time, or both. To examine the atmospheric drag effects, it is beneficial to analyze the apogee and perigee of the debris fragment orbits. Fig. 3 shows the apogee and perigee altitudes of the debris fragments over the propagation time for the Average ballistic coefficient case. Fig. 4, from the ODPO report, shows the apogee and perigee altitudes of the same debris fragments for the first three months of the year.

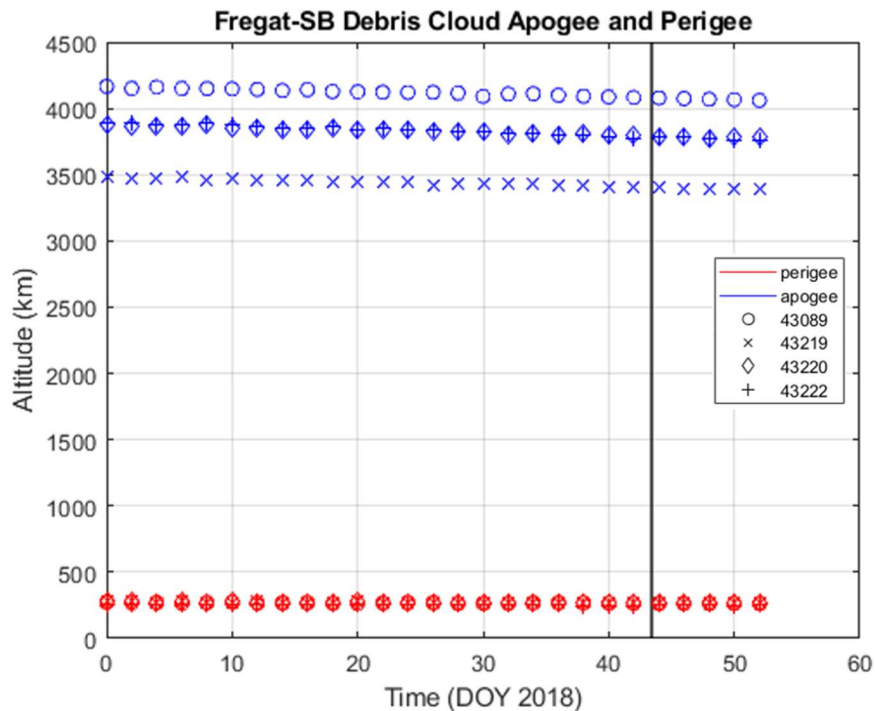


Figure 3: Orbital evolution of each debris fragment over propagation time. The results shown used the average case for ballistic coefficient calculation. Each debris fragment shows an approximate steady state of both apogee and perigee, with perigee almost unchanged between debris fragments. The line represents the ODPO reported actual time of event.

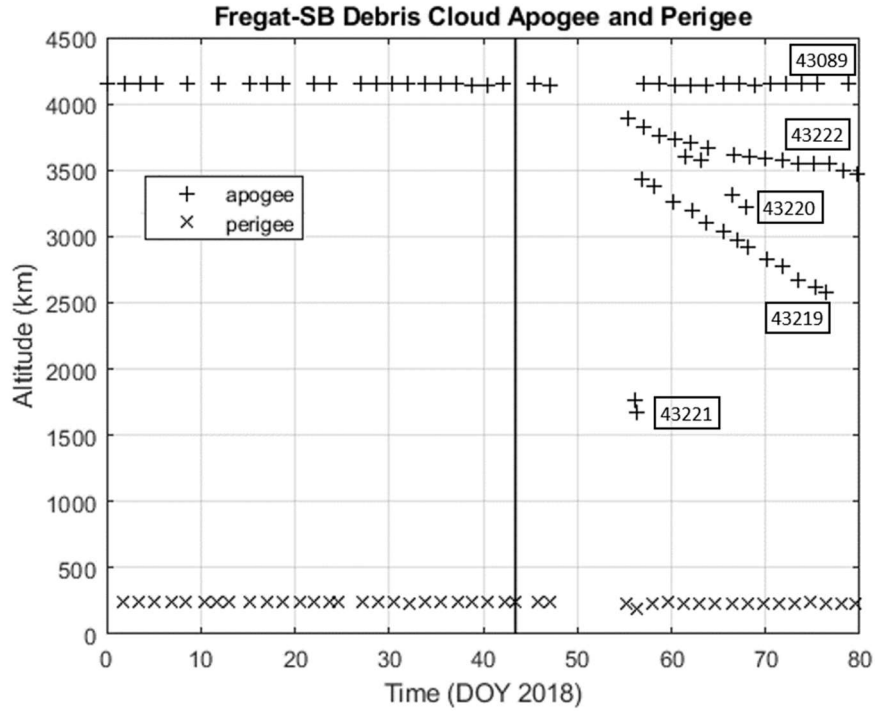


Figure 4: Orbital evolution of each debris fragment for the first 3 months of 2018. Data digitized and re-plotted from the ODPO report [2]. The line represents the ODPO reported actual time of event.

Fig. 3 shows an approximate steady state of apogee and perigee for all debris fragments, while Fig. 4 displays a drastic decrease in the apogee of all debris fragments, except debris fragment 43089, the original satellite re-categorized as a debris object. This decrease corresponds to a high rate of orbital decay, which is normally associated with a low ballistic coefficient and high A/m ratio. High A/m ratio objects are subject to marked radiation forces in addition to atmospheric drag. Retrospection of the A/m ratio of the debris fragments analyzed in this ballistic coefficient case (the Average case) shows that only one fragment had a relatively high A/m ratio, as seen in Table 4.

Table 4: A/m ratios calculated using the average ballistic coefficient for each debris fragment.

Debris SSN Number	Area-to-Mass Ratio [m ² /kg]
43089	0.0481
43219	0.8646
43220	0.4103
43222	174.9062

In Fig. 3, this high A/m ratio debris fragment displays a slight decrease in apogee over time, but nowhere near the rate of decay of the fragments shown in Fig. 4. This error indicates the need to continue researching the effects of the ballistic coefficient on orbit propagation, specifically on the A/m ratio as it impacts both solar radiation pressure and atmospheric drag effects. See Appendix A for the A/m ratios and calculated ballistic coefficients for all ballistic coefficient study cases. Appendix B shows the apogee/perigee plots for the 3-Sigma, Median, and None ballistic coefficient cases.

To examine the method of using the COM to identify the fragmentation time, it is beneficial to analyze the position of the debris fragments at the tool's identified fragmentation event time. Fig. 5 depicts the physical positions of the debris fragments at these times, and Table 5 shows the average distance to COM for that guess.

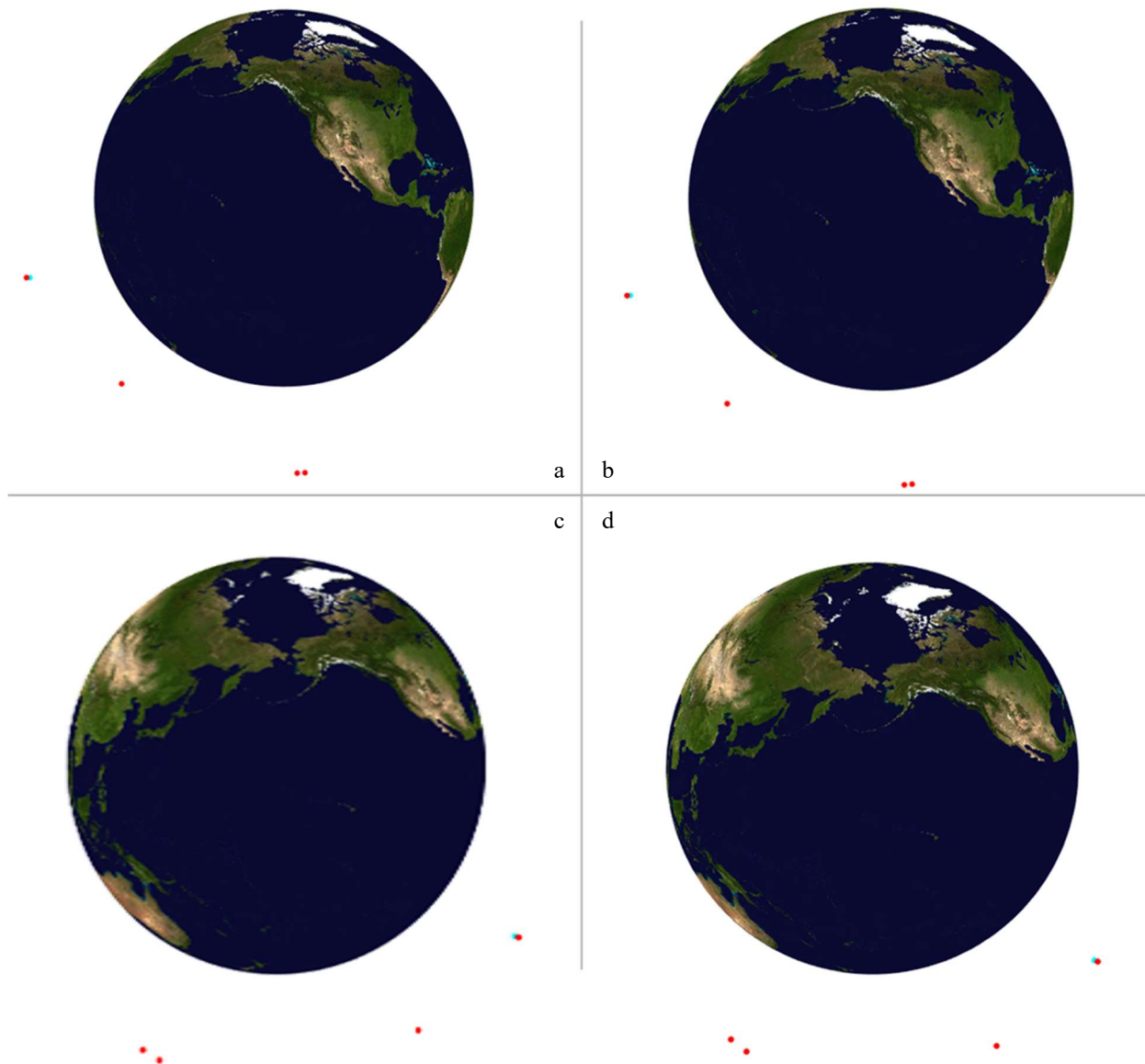


Figure 5: The position of the debris fragments at the calculated fragmentation event time for each case of ballistic coefficient calculation. The red dots each correspond to a debris fragment, while the light blue dot refers to the COM. Fig. 4a corresponds to the Average case, Fig. 4b to the 3-Sigma case, Fig. 4c to the Median case, and Fig. 4d to the case without drag.

Table 5: Average distances to the COM calculated for each ballistic coefficient case. Recall the i^{th} guess corresponds to the i^{th} smallest average distance to the COM for that case.

Ballistic Coefficient Case	Guess	Average Distance to COM [km]
Average	9	47.164
3-Sigma	9	47.164
Median	19	61.575
None	5	61.996

The positions of the debris fragments are much further from each other than expected for the fragments to be exploded debris from a parent object. This is likely due to the tool being unable to identify a parent satellite on the first guess, or at the minimum average distance to the COM. Calculating event time and location by minimizing the distance of

the fragments to each other, by using a particle distribution, or by comparing the propagated debris fragments with propagated satellite catalog objects may increase the accuracy of the tool. The error of the fragment locations indicates the need to continue researching the methods used to identify fragmentation events with more robust analysis techniques.

It is interesting to note that a higher guess value implies a higher error in the identification of the fragmentation event time and location, since the guess is getting further from the minimum average distance to the COM. However, Table 5 shows the smallest guess number, corresponding to the case without drag, results in the largest average distance to the COM, indicating the largest error. It is also apparent from this data that the Median case for ballistic coefficient calculation has a drastic effect on the accuracy of the tool, with its inability to identify the correct parent object or time and location of the fragmentation event, as well as its large average distance to COM value, rivaling that of the case which does not include atmospheric drag effects. This again indicates the need to continue researching the effects of the ballistic coefficient on orbit propagation, as well as a more efficient and accurate method of calculating the ballistic coefficient from TLE information.

9. CONCLUSION

This work presented a fragmentation event identification tool with the capability of identifying the origin of debris fragments from TLEs pulled from existing space surveillance networks. Physical analysis of the recent February 2018 Fregat-SB explosion correctly determined the parent satellite involved in the fragmentation event using back propagation and particle distribution techniques via COM calculation. Identifying the location and time of the fragmentation event proved more difficult with the current capabilities of the tool, with error possibly stemming from the A/m ratio calculation. This error may also be a result of the hypothesis that minimum average distance to the COM of the fragment cloud determines the time and location of the fragmentation event. Instead, a future study may include the forward propagation of nearby parent objects in their nominal orbit to calculate the distance between them and the cloud. Finding the minimum of this distance may better indicate the time and location of a fragmentation event. To further increase event identification accuracy, a future study will include statistical properties and their minimum variances. This may involve running multiple possibilities in a Monte Carlo analysis to determine fragmentation event time. The case study varying the ballistic coefficient calculation also provided some insight into how identifying the location and time of the fragmentation event may be remedied. In the future, additional research will be conducted to further understand the impact the ballistic coefficient has on the A/m ratio calculation, and therefore the effects of drag and solar radiation pressure. Variations on the solar radiation pressure coefficient may also be included in a future study.

10. REFERENCES

1. Dunbar, B. (2017, August 7). What Is Orbital Debris? (S. May, Ed.). Retrieved August 1, 2018, from <https://www.nasa.gov/audience/forstudents/5-8/features/nasa-knows/what-is-orbital-debris-58.html>
2. Andrișan, R. L., Ioniță, A. G., González, R. D., Ortiz, N. S., Caballero, F. P., & Krag, H. (2017). FRAGMENTATION EVENT MODEL AND ASSESSMENT TOOL (FREMAT) SUPPORTING ON-ORBIT FRAGMENTATION ANALYSIS. In *7th European Conference on Space Debris*.
3. Andrișan, R. L., López, N. G., Sánchez-Ortiz, N., & Flohrer, T. SST ANALYSIS TOOL (SSTAN) SUPPORTING SPACE SURVEILLANCE AND TRACKING (SST) SERVICES ASSESSMENT.
4. Itaya, Y., Fujita, K., & Hanada, T. (2018). Precise time estimation of on-orbit satellite fragmentations. *Acta Astronautica*.
5. Anz-Meador, P., & Shoots, D. (May 2018). Fragmentation of Fregat SB Upper Stage Debris. *Orbital Debris Quarterly News*, Volume 22 Issue 2.
6. Aly, A. F., Aly, M. N., Elshishtawy, M. E., & Zayan, M. A. (2002). Optimization techniques for orbit estimation and determination to control the satellite motion. In *Aerospace Conference Proceedings, 2002*. IEEE (Vol. 5, pp. 5-5). IEEE.
7. Vallado, D. A. (2013). *Fundamentals of astrodynamics and applications* (4th Ed). Springer Science & Business Media.
8. Joint Space Operations Center. (2018, August 23). Satellite Catalog. Retrieved August 9, 2018, from <https://www.space-track.org/>
9. Center for Space Standards and Innovation. (2018, August 23). EOP and Space Weather Data. Retrieved August 9, 2018, from <http://celestrak.com/SpaceData/>

10. Pilinski, M. D., Argrow, B. M., & Palo, S. E. (2011). Drag coefficients of satellites with concave geometries: comparing models and observations. *Journal of Spacecraft and Rockets*, 48(2), 312-325.
11. Anz-Meador, P., & Shoots, D. (April 2016). Fragmentation of Fregat Upper Stage Debris. *Orbital Debris Quarterly News*, Volume 20 Issue 1&2.
12. AGI STK. (2018, August). High-Precision Orbit Propagator (HPOP). Retrieved from <http://help.agi.com/stk/index.htm#hpop/hpop.htm>
13. Kelecy, T., Payne, T., Thurston, R., & Stansbery, G. (2007). Solar radiation pressure estimation and analysis of a GEO class of high area-to-mass ratio debris objects.
14. Picone, J. M., Hedin, A. E., Drob, D. P., & Aikin, A. C. (2002). NRLMSISE-00 empirical model of the atmosphere: Statistical comparisons and scientific issues. *Journal of Geophysical Research: Space Physics*, 107(A12), SIA-15.

APPENDIX A

Table 6: Epochs of the TLE for each debris fragment used for back propagation.

Debris SSN Number	TLE Epoch
43089	23 Feb 2018 15:47:52.198
43219	23 Feb 2018 12:06:01.267
43220	24 Feb 2018 23:31:52.835
43222	23 Feb 2018 02:52:04.308

Table 7: A/m ratios for each case of ballistic coefficient calculation for each debris fragment

Debris SSN Number	Area-to-Mass Ratio [m ² /kg]		
	Average BC	3-Sigma BC	Median BC
43089	0.0481	0.0194	1.0347e-06
43219	0.8646	0.8646	0.7887
43220	0.4103	0.4103	0.4081
43222	174.9062	174.9062	170.2399

Table 8: Ballistic coefficients for each case of calculation for each debris fragment

Debris SSN Number	Ballistic Coefficient [kg/m ²]		
	Average BC	3-Sigma BC	Median BC
43089	1.1906e+04	4.7911e+03	0.2554
43219	0.5153	0.5153	0.5649
43220	1.0859	1.0859	1.0916
43222	0.0025	0.0025	0.0026

APPENDIX B

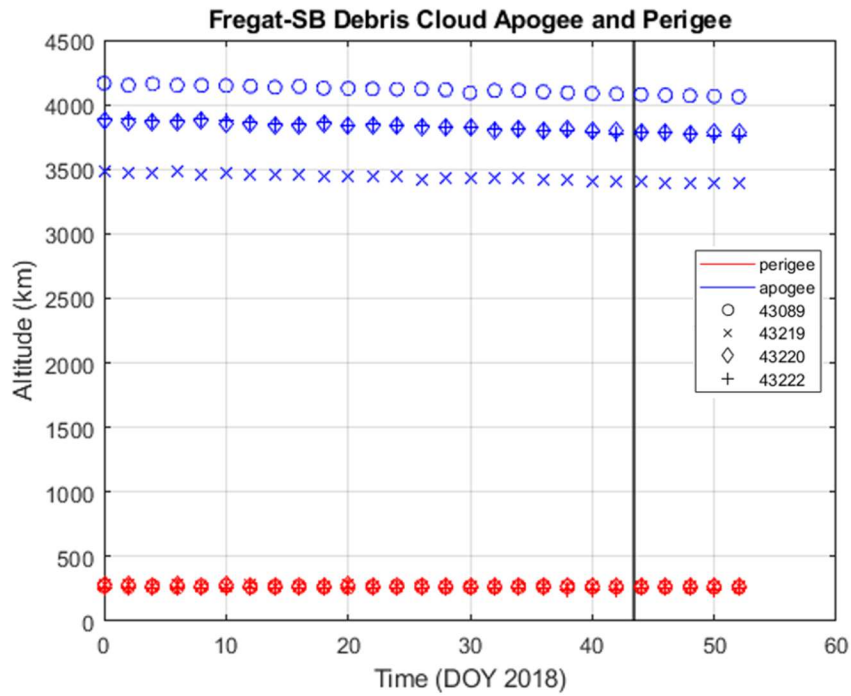


Figure 6: Orbital evolution of each debris fragment over propagation time. The results shown used the 3-Sigma case for ballistic coefficient calculation. The line represents the ODPO reported actual time of event.

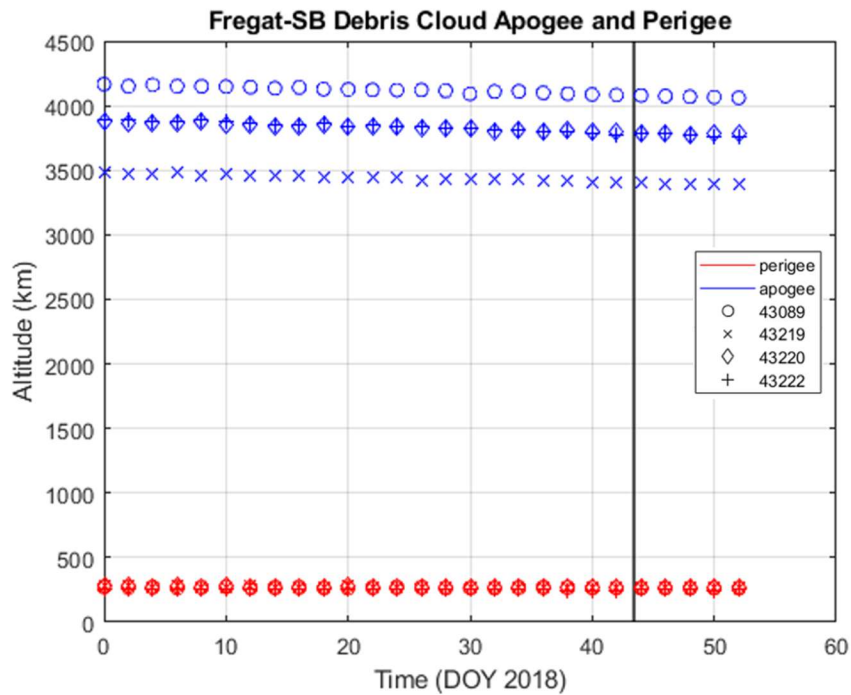


Figure 7: Orbital evolution of each debris fragment over propagation time. The results shown used the Median case for ballistic coefficient calculation. The line represents the ODPO reported actual time of event.

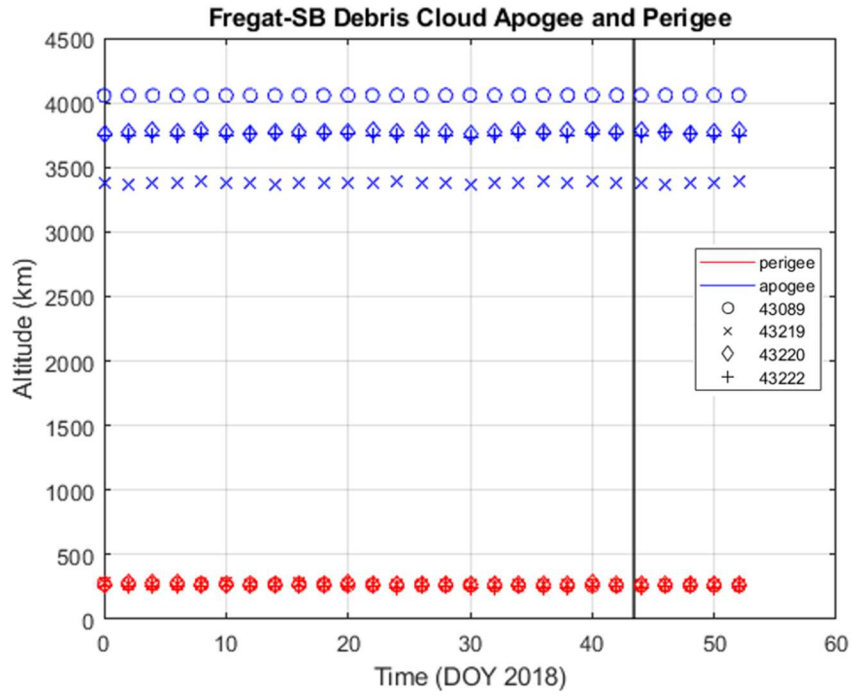


Figure 8: Orbital evolution of each debris fragment over propagation time. The results shown used the case with no ballistic coefficient calculated and no drag effects. The line represents the ODPO reported actual time of event.